A simple 3D model for coastal and estuarial applications

J. Osment

ABSTRACT

This paper describes a 3D model that was constructed in response to the need for a simple model for use in coastal and estuarial applications where tidal range may be large in relation to water depth. The model was required to simulate density driven flows. The model configuration selected to meet these objectives is presented, together with the assumptions, formulation and solution techniques upon which the model is based. The validation of the model against analytical results, an empirical relationship and other model results are also described.

Key words | 3D, numerical model, tidal range, density flows

J. Osment
Halcrow Group,
Burderop Park,
Swindon,
Wilts SN4 0QD
UK
E-mail: *OsmentJ@halcrow.com*

INTRODUCTION

The layered model DAWN3D was developed as an economical alternative to a full 3D model for use in typical engineering applications, where vertical velocities are small in relation to horizontal velocities. Since the model was intended for use in coastal and estuarine applications, it was essential that it was able to handle the wetting and drying of the intertidal areas within the computational domain, without being limited by the tidal range of the application.

With the assumption of small vertical velocities and with fluid pressure being taken as due to hydrostatic pressure alone, the formulation reduces to the depth-integrated continuity equation for incompressible flow and the horizontal Navier–Stokes equations over each layer. The equations are solved with an Alternating Direction Implicit scheme to yield the horizontal and vertical velocities in each layer. A simple two-equation mixing length turbulence model is used.

By definition the processes of wetting and drying are confined to the first layer. With a system in which the layer numbers are fixed to prescribed levels, the thickness of the top layer would therefore be defined by the tidal range. In areas of large tidal range this would not be acceptable. However, if a regular vertical mesh is used it becomes possible (over the relatively small study areas envisaged for this model) to re-number the layers according to the instantaneous water level, so that the layer boundaries maintain their level, but change their numbering to keep the water surface in the uppermost layer. In this way the thickness of the top layer is not controlled by the tidal range at the site modelled.

The model was therefore formulated on a square horizontal grid, with a vertical grid system in which the layers are level, of equal thickness and have their boundaries at fixed levels to allow the re-assignment and re-numbering of the layers as appropriate to correspond to changes in water level. The notation used in the grid and coordinate system is shown in Figure 1.

METHODS

Model formulation

The hydrostatic pressure assumption is expressed as

$$\frac{\partial P}{\partial z} + \rho g = 0 \tag{1}$$

where P is the pressure. With the assumption of small vertical velocities the continuity equation and the horizontal momentum equations may then be written as

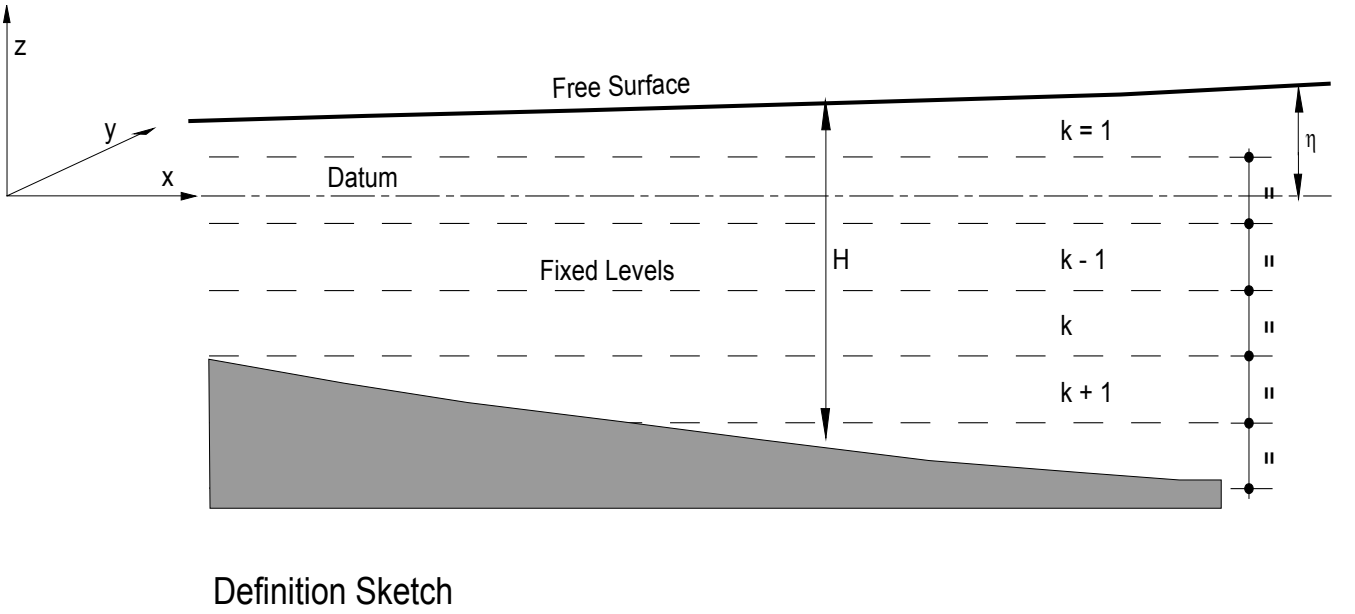

Figure 1 | Definition sketch.

$$\frac{\partial u}{\partial x}+\frac{\partial v}{\partial y}+\frac{\partial w}{\partial z}=0 \tag{2}$$

$$\frac{\partial u}{\partial t}+\frac{\partial uu}{\partial x}+\frac{\partial uv}{\partial y}+\frac{\partial uw}{\partial z}=fv - \frac{1}{\rho}\frac{\partial P}{\partial x}+\frac{1}{\rho}\left[\frac{\partial \sigma_{xx}}{\partial x}+\frac{\partial \tau_{xy}}{\partial y}+\frac{\partial \tau_{xz}}{\partial z}\right] \tag{3}$$

$$\frac{\partial v}{\partial t}+\frac{\partial vu}{\partial x}+\frac{\partial vv}{\partial y}+\frac{\partial vw}{\partial z}=-fu - \frac{1}{\rho}\frac{\partial P}{\partial y}+\frac{1}{\rho}\left[\frac{\partial \tau_{yx}}{\partial x}+\frac{\partial \sigma_{yy}}{\partial y}+\frac{\partial \tau_{yz}}{\partial z}\right] \tag{4}$$

where t is time; x, y are Cartesian coordinates in the horizontal plane; z is the Cartesian coordinate in the vertical (measured upwards); u, v, w are components of velocity in the x, y, z directions, respectively; η is the z value at the surface; g is the acceleration due to gravity; p is pressure; ρ is fluid density; f is the Coriolis parameter; and σ_{xx}, σ_{yy}, τ_{xy}, τ_{xz}, τ_{yx}, τ_{yz} are the components of Reynolds stress.

Integration of the continuity equation over layer k gives

$$w_{k-1/2}-w_{k+1/2}+\frac{\partial(hu_k)}{\partial x}+\frac{\partial(hv_k)}{\partial y}=0 \tag{5}$$

where u_k and v_k are the layer averaged velocities, h is the layer thickness and $w_{k-1/2}$ and $w_{k+1/2}$ are vertical velocities on the layer boundaries.

If the continuity equation is integrated over the full water depth, Equation (5) reduces to

$$\frac{\partial \eta}{\partial t}+\frac{\partial HU}{\partial x}+\frac{\partial HV}{\partial y}=0 \tag{6}$$

where U and V are the depth averaged velocities and H is the water depth.

Reynolds stresses in the x direction are evaluated from the Boussinesq formulation as

$$\sigma_{xx}=\rho\varepsilon_h\left[\frac{\partial u_k}{\partial x}+\frac{\partial u_k}{\partial x}\right]$$
$$\tau_{xy}=\rho\varepsilon_h\left[\frac{\partial u_k}{\partial y}+\frac{\partial v_k}{\partial x}\right] \tag{7}$$
$$\tau_{xz}=\rho\varepsilon_v\left[\frac{\partial u_k}{\partial z}+\frac{\partial w_k}{\partial x}\right]$$

where the horizontal eddy diffusivity ε_h is taken as constant, and the vertical eddy diffusivity ε_v is evaluated from a two-layer mixing length model as

$$\varepsilon_v = l^2 \left[\left(\frac{\partial u_k}{\partial z} \right)^2 + \left(\frac{\partial v_k}{\partial z} \right)^2 \right]^{1/2}. \tag{8}$$

The mixing length l is taken, after Lin & Falconer (1997), as

$$l = \varkappa Z \text{ for } \varkappa Z \leq 0.1H \tag{9}$$

$$l = 0.1H \text{ for } \varkappa Z > 0.1H$$

where H is the water depth, Z is the distance up from the bed and $\varkappa$ is Von Karman's constant ($=0.41$).

The y direction stresses are computed similarly.

Integration of the momentum equations over layer k then leads to

$$\frac{\partial p_k}{\partial t} + \frac{\partial u_k p_k}{\partial x} + \frac{\partial v_k p_k}{\partial y} = f q_k - \frac{h}{\rho}\frac{\partial P}{\partial x} + \frac{\partial}{\partial x}\left(\varepsilon_h h \left[\frac{\partial u_k}{\partial x} + \frac{\partial u_k}{\partial x} \right] \right) + \frac{\partial}{\partial y}\left(\varepsilon_h h \left[\frac{\partial u_k}{\partial y} + \frac{\partial v_k}{\partial x} \right] \right) + (wu)_{k+1/2} - (wu)_{k-1/2} + \frac{1}{\rho}[\tau_{xz_{k-1/2}} - \tau_{xz_{k+1/2}}] \tag{10}$$

$$\frac{\partial q_k}{\partial t} + \frac{\partial u_k q_k}{\partial x} + \frac{\partial v_k q_k}{\partial y} = -f p_k - \frac{h}{\rho}\frac{\partial P}{\partial y} + \frac{\partial}{\partial x}\left(\varepsilon_h h \left[\frac{\partial v_k}{\partial x} + \frac{\partial u_k}{\partial y} \right] \right) + \frac{\partial}{\partial y}\left(\varepsilon_h h \left[\frac{\partial v_k}{\partial y} + \frac{\partial v_k}{\partial y} \right] \right) + (wv)_{k+1/2} - (wv)_{k-1/2} + \frac{1}{\rho}[\tau_{yz_{k-1/2}} - \tau_{yz_{k+1/2}}] \tag{11}$$

where p_k ($=u_k h$) and q_k ($=v_k h$) are unit layer discharges in the x and y directions, respectively. When applied to the whole depth, the layer thickness h is replaced by the water depth H; the terms $(wu)_{k+1/2}$ and $(wv)_{k+1/2}$ are eliminated by the zero flow boundary conditions at the bed ($k_{bed}+\frac{1}{2}$), and the terms $(wu)_{k-1/2}$ and $(wv)_{k-1/2}$ are replaced at the surface ($k=\frac{1}{2}$) by $\mathrm{d}\eta/\mathrm{d}t(u)_{k=1/2}$, $\mathrm{d}\eta/\mathrm{d}t(v)_{k=1/2}$. The horizontal shear stress terms $\tau_{k-1/2}$ and $\tau_{k+1/2}$ are replaced by terms for the wind shear stress at the surface and the bed shear stress at the bottom, respectively.

The bed shear stress is evaluated as

$$\frac{\tau_{bed_x}}{\rho} = u_b \sqrt{u_b^2 + v_b^2} \left[2.5 \ln\left(\frac{13.2d}{k_s} \right) \right]^{-2} \tag{12a}$$

$$\frac{\tau_{bed_y}}{\rho} = v_b \sqrt{u_b^2 + v_b^2} \left[2.5 \ln\left(\frac{13.2d}{k_s} \right) \right]^{-2} \tag{12b}$$

where u_b and v_b are the layer average velocity components in the bottom layer, d is the thickness of the bottom layer and k_s is the roughness length.

The layer averaged equation for transport and diffusion of a solute may be written as

$$\frac{\partial h C_k}{\partial t} + h\left[\frac{\partial u_k C_k}{\partial x} + \frac{\partial v_k C_k}{\partial y} \right] + (wC)_{k-1/2} - (wC)_{k+1/2} = \left[\frac{\partial}{\partial x}\left(h\delta_x \frac{\partial C_k}{\partial x} \right) + \frac{\partial}{\partial y}\left(h\delta_y \frac{\partial C_k}{\partial y} \right) + \frac{\partial}{\partial z}\left(h\delta_z \frac{\partial C_k}{\partial z} \right) \right] + Q \tag{13}$$

where C_k is the layer averaged solute concentration, Q is a layer averaged source term and δ_x, δ_y and δ_z are layer averaged diffusion coefficients. Following the form adopted by Falconer (1986), the horizontal layer averaged coefficients were taken as

$$\delta_x = \frac{(k_l u_k^2 + k_t v_k^2)\, H\sqrt{g}}{C_{Chezy}\left(\sqrt{u_k^2 + v_k^2}\right)}$$

$$\delta_y = \frac{(k_l v_k^2 + k_t u_k^2)\, H\sqrt{g}}{C_{Chezy}\left(\sqrt{u_k^2 + v_k^2}\right)} \tag{14}$$

where $C_{Chèzy}$ is the Chèzy friction coefficient, taken as

$$C_{Chèzy} = 18 \log(13.2H/k_s) \tag{15}$$

and k_l and k_t are, respectively, the longitudinal and transverse depth mean diffusion coefficients, with values taken as 5.93 and 0.15, respectively (Fischer 1973).

The vertical diffusion coefficient δ_z is evaluated according to the method described by Odd & Roger (1978).

Fluid density is obtained as a function of temperature and salinity from the International Equation of State of Sea Water, 1980 (IES80, Unesco 1981).

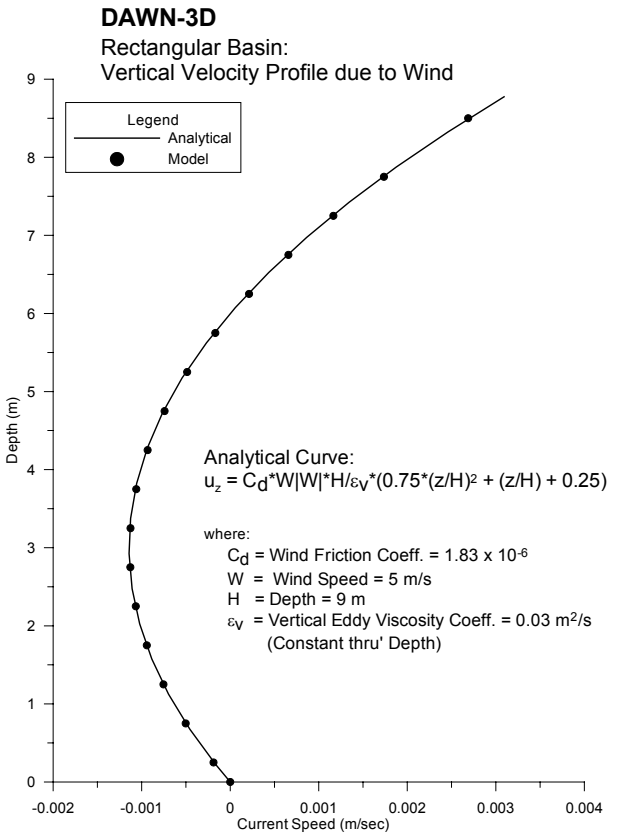

Figure 2 | DAWN-3D. Rectangular basin: vertical velocity profile due to wind.

Solution method

The first step in the solution at each time step is the solution of the depth averaged equations (6), (10) and (11) over the full water depth to evaluate the free surface level η. The convective terms in Equations (10 and (11) are handled by application of the 'SuperBee' TVD scheme (James 1996) and a conventional ADI approach is used.

Once the surface level η is defined, the layer averaged Equations (5), (10) and (11) may be solved in turn for vertical velocities and layer averaged horizontal velocities by starting at the bottom, where vertical velocity across the bottom boundary is zero. Again, the 'SuperBee' TVD scheme is used to formulate the convective terms and an ADI scheme is used to solve the equations. The computed horizontal layer velocities are used to update the depth averaged velocities at this stage.

The horizontal and vertical velocities obtained from the solution of the layer averaged equations are then used for solution of Equation (13) to obtain layer averaged values of solute concentration. The 'SuperBee' TVD scheme is again used in the formulation of the convective terms in Equation (13). For simplicity this is solved explicitly. No stability problems have been noted in connection with the use of the explicit solution. The values of parameter concentration obtained from the solution of Equation (13) are next used to evaluate the water density by application of IES80. (If salinity or temperature alone is represented, appropriate values of the non-simulated parameter must be assumed for solution of IES80.) The computed values of water density are then used for the hydrodynamic solution in the following time step.

MODEL VALIDATION

The model has been validated against three independent data sets, as follows:

1. an analytical solution for wind-induced velocities,
2. an empirically derived relationship for initial dilution,
3. other 3D model results for a hypothetical geostrophic adjustment.

Wind-induced vertical profile

The hydrodynamic solution was first compared with the theoretical vertical velocity profile produced by the action of wind shear stress on the water surface. By assuming a constant value for vertical eddy diffusivity ε_v the horizontal velocity at a distance z above the surface may be expressed (after Matsoukis & Papadopolis-Dezorzis 1992) as

$$u = \frac{\rho_{air}}{\rho} C_{star} \left| W \right| W \frac{H}{\varepsilon_v} \left[0.75 \left(\frac{z-\eta}{H} \right)^2 + \frac{z-\eta}{H} + 0.25 \right] \text{for} -1 \le \left(z - \eta/H \right) \le 0 \quad (16)$$

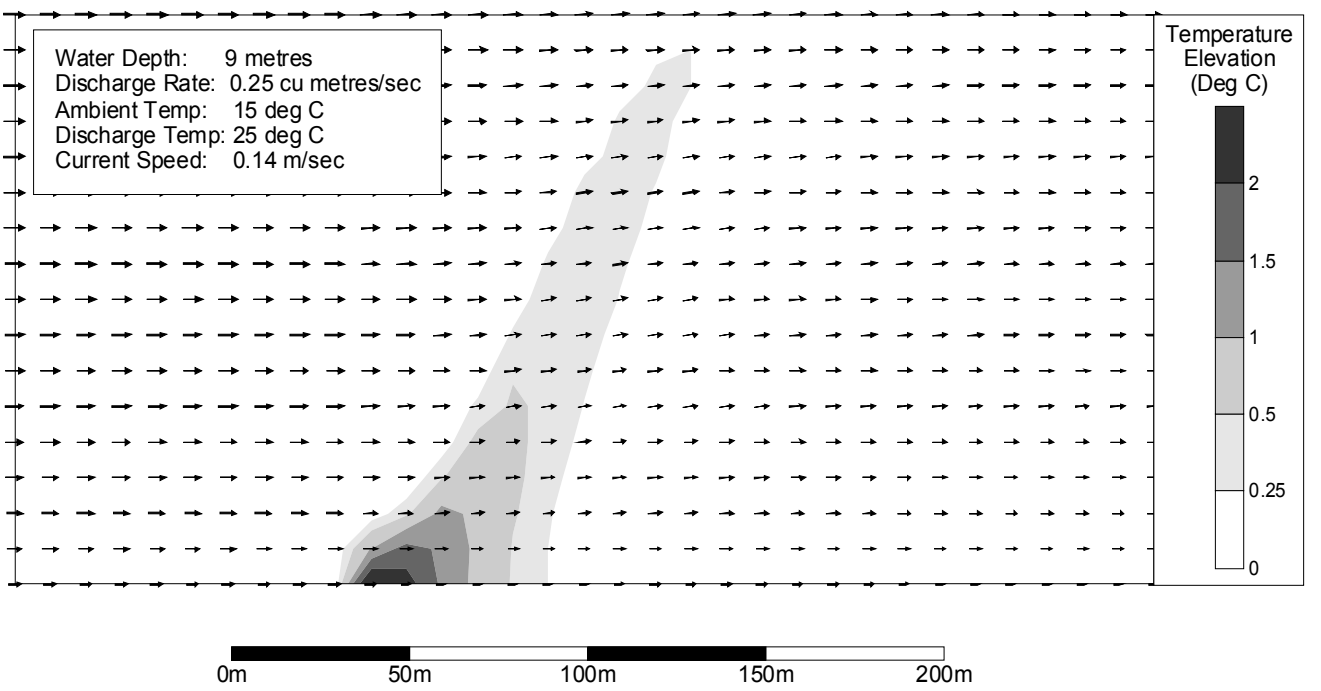

Figure 3 | Initial dilution test.

where W is the wind speed, ρ_{air} is the density of air and C_{star} is a coefficient taken as 0.0015.

To test the model against this analytical result the model was set up to represent a straight, level channel 280 m wide, 9 m deep and 1,000 m long, with closed ends. Grid mesh sizes of 10 m and 0.5 m were used in the horizontal and vertical, respectively. With the vertical eddy diffusivity constant through the water column, as required for compatibility with the analytical result, the model was not stable at Courant numbers above 2.8 (equivalent to a time step of 3 sec). Reducing the time step below 3 sec caused less than 0.1% variation in the results obtained for horizontal velocity.

The vertical current profile predicted by the model for a wind speed of 5 m/sec is shown plotted against the analytical profile computed from Equation (16) in Figure 2.

A good agreement is apparent between the analytical results and the velocity profile predicted by the model. But the assumptions made in the analytical solution relating to the governing physical processes (such as a constant eddy viscosity) are capable of exact reproduction in the model. Therefore, whilst this comparison is an effective test of the model formulation and solution, it is not necessarily a reliable test of the model's ability to simulate natural processes.

Initial dilution

The second test carried out on the model involved a study of the initial dilution of a buoyant plume from a continuous discharge on the bed, in which the model results were compared with those of an empirical model.

The model was set up to represent a straight, level channel of rectangular cross section, with depth = 9 m, width = 280 m and length = 1 km. A horizontal grid mesh size of 10 m was used in conjunction with a layer thickness of 1 m and a time step of 1 sec. Flows and water surface elevations were prescribed at upstream and downstream boundaries, respectively. The model was arranged

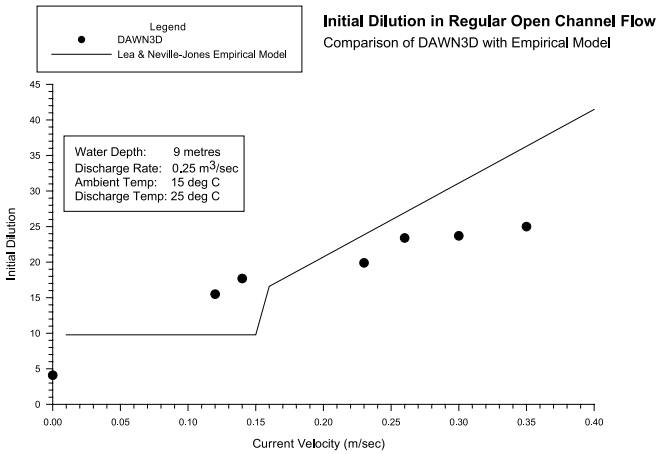

Figure 4 | Initial dilution in regular open channel flow.

to simulate a continuous bottom discharge of thermal effluent with a temperature elevation (above ambient) of 10°C from an outfall sited 200 m from the upstream boundary. The model arrangement is shown in Figure 3. The test was repeated for a range of different flow velocities. For each flow velocity the minimum initial dilution was computed as the ratio of temperature elevation at the point of discharge against the maximum temperature elevation in the surface boil.

The initial dilutions predicted by the model are shown plotted against those predicted by the Lee & Neville-Jones empirical model (Lee & Neville-Jones 1987) in Figure 4. Generally there is good agreement between the model results and the Lee & Neville-Jones

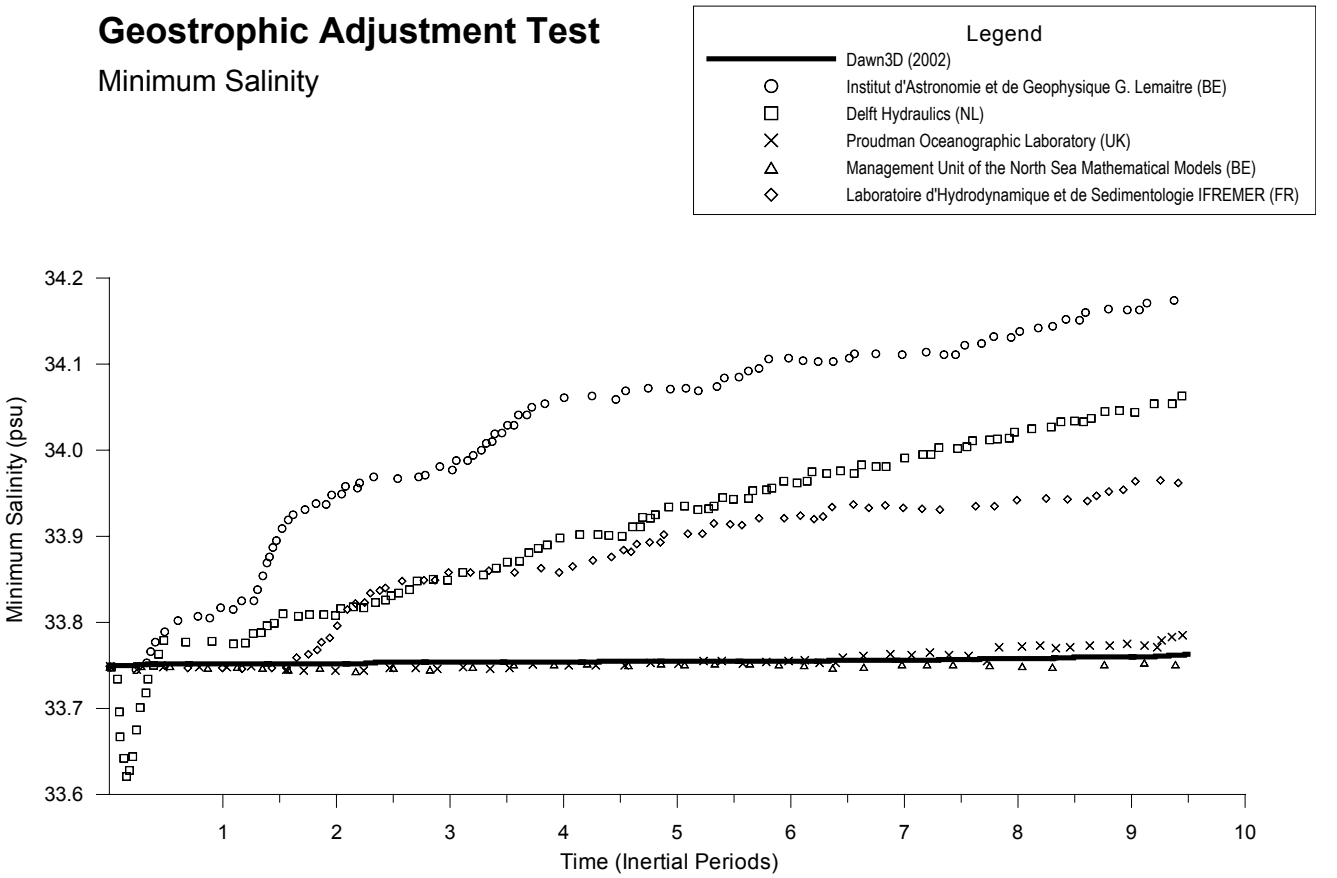

Figure 5 | Geostrophic adjustment test: minimum salinity.

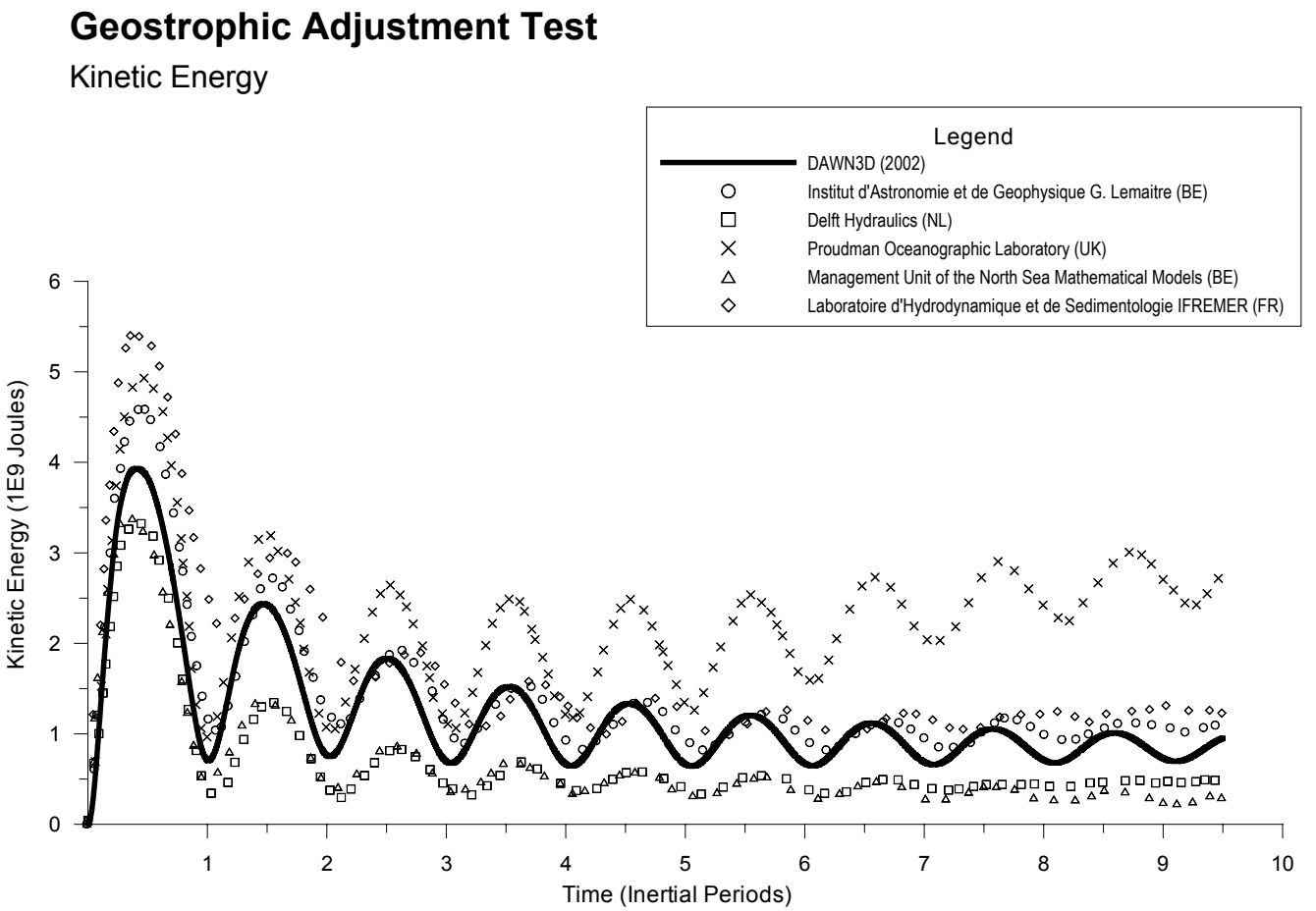

Figure 6 | Geostrophic adjustment test: kinetic energy.

empirical relationship over the range of velocities tested, but there is also some indication that the initial dilutions being predicted by the model are diverging from those predicted by the empirical model at higher flow velocities. One possible cause of this variation could be the limitations of the simple turbulence model adopted in the present formulation. More advanced turbulence closures have yet to be tested.

Geostrophic adjustment test

The third validation test on the model involved comparison with several well-established 3D models by reference to a study by Tartinville *et al.* (1998) in which five such models were applied to a standard (hypothetical) test case to simulate the geostrophic adjustment of a cylinder of reduced density.

If a cylinder of reduced salinity were to be introduced into an ambient saline environment the cylinder would initially rise, and would thereafter oscillate vertically. The cylinder of reduced density would attract flows towards the centre of the cylinder at lower levels and cause a corresponding outward flow at upper levels. In the absence of any other driving forces, the effect of Coriolis forces on these flows would be to generate a clockwise surface eddy (in the Northern hemisphere). This is the hypothetical scenario posed for this test, whose specification includes the removal of all fluid damping from the system. The values of parameters such as total kinetic energy, and total available potential energy will oscillate with the vertical oscillation of the cylinder.

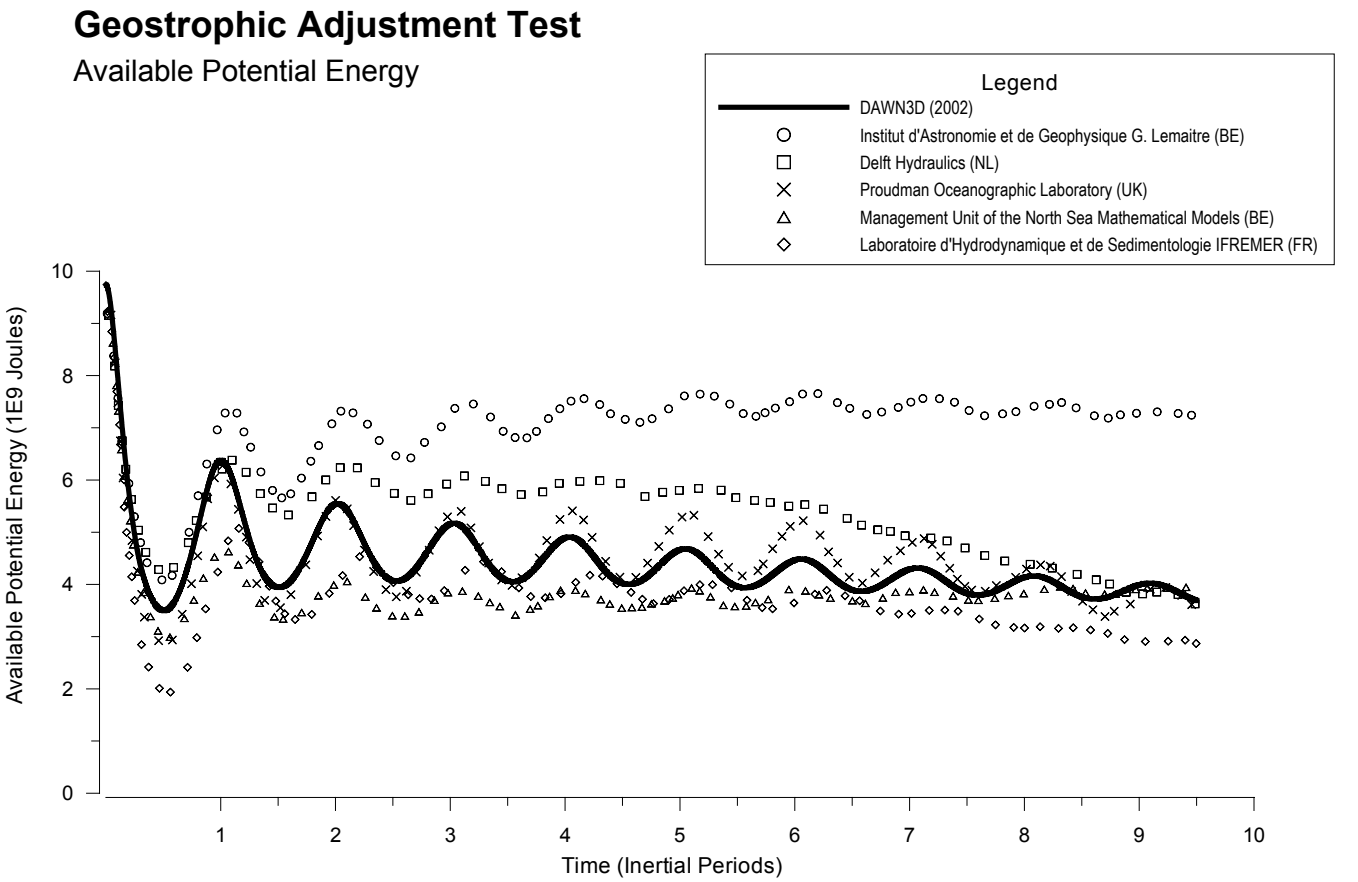

Figure 7 | Geostrophic adjustment test: available potential energy.

This test was selected because it was the basis of the test adopted by Tartinville *et al.* (1998) to compare a set of selected 3D models. A 10 m deep cylinder of reduced density was introduced into a saline water environment of depth 20 m. The initial value of salinity in the cylinder was 33.75 psu (compared to an ambient value of 34.85 psu). All viscous forces were removed from the models and the resulting vertical oscillation of the cylinder produced variations in total kinetic energy and total available potential energy that were used as the basis for comparing the models. The dimensions and mesh size of the model to be used for this test were defined by the test specifications as 30 km and 1 km, respectively, with the cylinder of reduced density having a diameter of 6 km. A layer thickness of 1 m was used, with a time step of 30 sec.

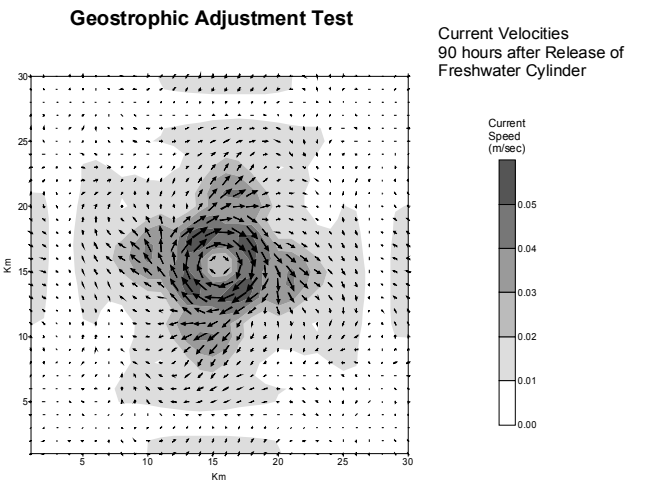

Figure 8 | Geostrophic adjustment test: curreny velocities 90 h after release of freshwater cylinder.

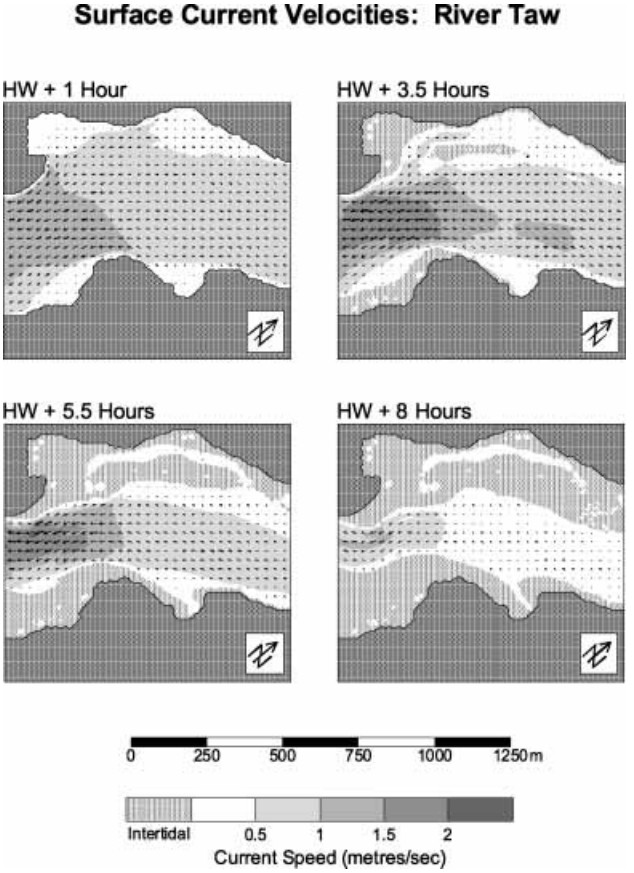

Figure 9 | Surface current velocities: River Taw.

In the absence of numerical diffusion the initial (reduced) value of salinity at the centre of the cylinder should be preserved until the effects of turbulent mixing become manifest. The variation of the minimum value of salinity with time is therefore an indicator of the degree of numerical diffusion in the solution.

The minimum value of salinity computed by the present model is presented in Figure 5 with the corresponding results from the other models shown for comparison. The variation of total kinetic energy and total available potential energy with time for the five existing models and for DAWN3D are shown in Figures 6 and 7. Figure 8 shows the surface current pattern at 90 h after release of the cylinder.

From Figure 5, the relative lack of corruption of the original value of the reduced salinity suggests a lower level of numerical diffusion than most of the other models. The precision of this result is attributed to the TVD treatment of the advective terms in both the hydrodynamic and pollutant transport formulations.

Of the other models tested, the model from Proudman Oceanographic Laboratory (POL) is perceived by Tartinville *et al.* (1998) to produce the most accurate results. There is good agreement between the potential energy results predicted by the present model and the equivalent results from the POL model, in terms of both the magnitude of total potential energy and the frequency of oscillation. However, the predictions of kinetic energy from the POL model differs from all the other models (including the present model) in that kinetic energy is shown increasing with time, suggesting that all the other models could be losing energy, presumably across the boundaries.

WETTING AND DRYING

The methodology adopted to handle tidal ranges greater than the model layer thickness was tested by application of the model to the River Taw in southwest England. In the area around Yelland this river has a tidal range of 7 m, with a maximum water depth of approximately 9 m. Peak current velocities exceed 2 m/sec. This application therefore tests not only the ability of the model to handle a large tidal range but also represents a good test of the stability of the model under severe real conditions involving high current speeds and the need to simulate the wetting and drying of extensive intertidal areas.

The model was set up with a horizontal mesh size of 10 m and a layer thickness of 1 m. It was driven by an existing, previously proven, depth averaged model of the rivers Taw and Torridge extending to Barnstaple and Weare Giffard, respectively, and having a grid mesh size of 60 m. Model cells are considered to dry, and are removed from the computation, when the water depth on all four sides is reduced below a predefined critical depth (set at 200 mm). Dry cells are allowed to flood when, on any cell side, the water level in the contiguous cell exceeds that of the dry cell and there is a water depth between the cells greater than the predefined critical depth.

Figure 9 shows the surface current vectors at various stages in the ebb tide for a spring tide with a range of 7 m. The extensive intertidal area is clearly seen and demonstrates the ability of the model to handle the large tidal range for which it was designed.

CONCLUSIONS

The simple layer averaged semi-3D model whose construction and validation is described here is able to reproduce with an acceptable level of accuracy the initial dilution processes in moderate current speeds, although the accuracy in higher current speeds is as yet unproven.

When compared with a set of contemporary 3D models from other modelling institutions, the present model is shown to compete very effectively.

Evidence has been presented that demonstrates the ability of the model to simulate an onerous 'real world' situation involving high current speeds and a tidal range that is large in relation to the water depth and the model layer thickness.

NOMENCLATURE

$C_{Chèzy}$ = Chèzy friction coefficient
C_k = layer averaged solute concentration
C_{star} = coefficient taken as 0.0015
d = bottom layer thickness
f = Coriolis parameter
g = gravitational acceleration
h = layer thickness
H = water depth
k = layer number
k_l, k_t = longitudinal and transverse depth mean diffusion coefficients
k_s = roughness length
l = mixing length
p_k, q_k = unit layer discharges in x, y
P = pressure.
Q = layer averaged source term
t = time
u, v, w = velocity components in the x, y, z directions
u_b = bottom layer average velocity
u_k, v_k = layer averaged velocities
U, V = depth averaged velocities
W = wind speed
x, y, z = Cartesian coordinates
δ_x, δ_y, δ_z = layer averaged diffusion coefficients
ε_h = horizontal eddy diffusivity
ε_v = vertical eddy diffusivity
$\eta = z$ value at surface (surface elevation)
$\varkappa$ = Von Karman's constant ($= 0.41$).
ρ = fluid density
ρ_{air} = air density
σ_{xx}, σ_{yy}, τ_{xy}, τ_{xz}, τ_{yx}, τ_{yz} = components of Reynolds stress.

REFERENCES

Fischer, H. B. 1973. Longitudinal dispersion and turbulent mixing in open-channel flow. *Ann. Rev. Fluid Mech.* **5**, 59–78.

James, I. 1996. Advection schemes for shelf sea models. *J. Marine Syst.* **8**, 237–254.

Lee, J. H. W. & Neville-Jones, P. 1987. Initial dilution of horizontal jet in crossflow. *J. Hydraul. Engng.* **113** (5), May.

Lin, B. & Falconer, R. A. 1997. Three-dimensional layer-integrated modelling of estuarine flows with flooding and drying. *Estuarine, Coastal Shelf Sci.* **44**, 737–751.

Matsoukis, M. & Papadopolis-Dezorzis, A. 1992. Three-dimensional characteristics model of wind-generated turbulent flow. *J. Engng. Mech. ASCE* **118** (8), 1526–1545.

Odd, N. V. M. & Roger, J. G. 1978. Vertical mixing in stratified tidal flows. *J. Hydraul. Div. ASCE* **104** (HY3), 337–351.

Falconer, R. A. 1986. Water quality simulation of a natural harbour. *J. Waterway, Port, Coastal Ocean Engng.* **112** (1), 15–34.

Tartinville, B., Deleersnijder, E., Lazure, P., Proctor, R., Ruddick, K. G. & Uittenbogaard, R. E. 1998. A coastal ocean model intercomparison study for a three-dimensional idealised test case. *Appl. Math. Model.* **22**, 165–182.

UNESCO. 1981. *UNESCO Technical Paper in Marine Science* No. 36.